Computational Modeling of Azobenzenes for Optically Addressable Liquid Crystal Alignment

Kyle Xiao

Webster Schroeder High School

Webster, NY

Advisor: Kenneth L. Marshall

Laboratory for Laser Energetics

University of Rochester

Rochester, NY

December 2014

Abstract

Photoisomerization of azobenzene between its rod-like *trans* and bent *cis* forms can be used to control liquid crystal alignment. This property makes azobenzenes useful in optically addressable liquid crystal beam shapers. Rather than using the costly trial-and-error synthesis method to synthesize a large array of compounds in order to identify unique characteristics of certain azobenzenes, computational modeling was performed. Density functional theory (DFT) and time-dependent DFT calculations were performed in this study using Schrodinger's Materials Science Suite to model azobenzenes tethered to a polymer backbone. The length of the spacer chain tethering the azobenzene to the polymer was shown to affect the energy difference between the *trans* and *cis* states. The addition of terminal groups was also explored and yielded interesting results. A cyanate ester terminal group increased the energy difference between isomers by 50% and 2-methoxy-N-(2-methylphenyl) acetamide group decreased the energy difference by 75%. Adding terminal groups tended to increase the wavelength of light required to initiate *trans-cis* isomerization. The addition of terminal groups also resulted in fluctuations in the HOMO-LUMO bandgap.

1. Introduction

Azobenzenes are defined by the double bond between the two nitrogens at their centers. Composed of two phenyl rings along with a nitrogen double bond, azobenzenes are noted for their ability to *photoisomerize* (i.e., photomechanically switch between the rod-like *trans* isomer and the bent *cis* isomer) when irradiated with the appropriate wavelength of UV or visible light. Under UV irradiation, *trans-cis* isomerization is initiated, whereas *cis-trans* isomerization occurs when the material is exposed to visible region light of the appropriate intensity (Fig. 1).

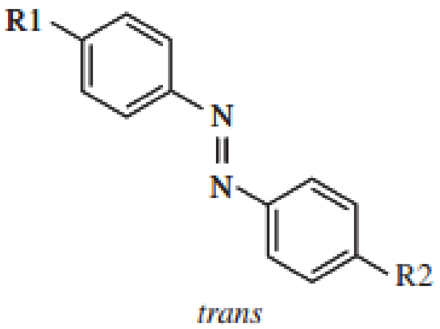

Fig. 1: Photochemically induced isomerization of azobenzene derivatives. R_1 and R_2 are terminal groups.

Beam shaping is required in high-peak-power laser systems for a variety of applications. The beam shapers currently used in OMEGA EP are composed of metal pixels deposited on a fused silica substrate.[1] Once the pattern has been generated, it cannot be changed; a new beam shaper needs to be fabricated. These metal-mask beam shapers are also limited to only the lowest-fluence areas of OMEGA EP due to their low laser damage threshold (250-500 mJ/cm^2 at 1054 nm, 1 ns pulse width). Electro-optical liquid crystal (LC) programmable spatial light modulators (PSLIM's) are also used in OMEGA EP to actively control the beam profile, but these devices suffer from the same low damage threshold as metal mask beam shapers due to the need for conductive-oxide electrodes required for their operation. A new alternative to these beam shapers would be an LC beam shaping device similar to the PSLIM except that the conductive oxide electrodes are replaced with a photoswitchable alignment coating composed of azobenzene "pendants" tethered to a polymer backbone. Because LC molecules are anisotropic in shape, they can exhibit differing optical properties depending on the direction light is incident on the molecular structure. This difference in optical properties can be used to modulate or attenuate the intensity or phase of a light beam that is incident on the LC material or device. The major axes of the liquid crystals have a tendency to align with long axes of the azobenzene pendants, and will change their orientation in response to a change in the orientation of the azobenzene pendants as they undergo photoinduced *trans*-*cis* (and *cis*-*trans*) isomerization, resulting in an optically-induced change in the intensity or phase of the incident light. Figure 2 shows the molecular reorientation of LC molecules in contact with photoswitchable alignment layer that are designed to produce LC reorientation either out-of-plane (Fig 2, top) or in-plane (Fig 2, bottom) with respect to the device substrates. Testing at LLE has demonstrated that these azobenzene alignment layers have 1054-nm laser damage thresholds ranging from 28 to 67 J/cm^2 at 1054 nm, 1 ns pulse width, which is well above the minimum requirement to be a viable alternative to the currently used PSLIM beam shapers.[2]

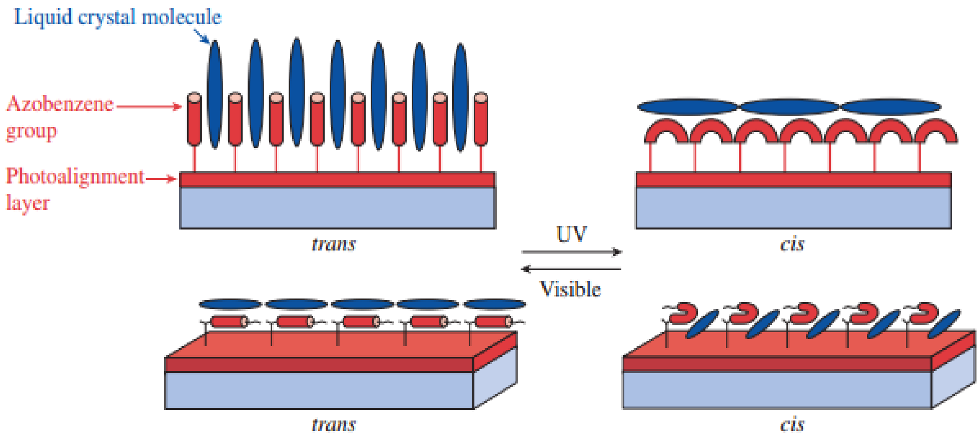

Fig. 2: Optically-addressed switching of LC devices using photoswitchable azobenzene alignment layers designed to induce out of plane (top) or in-plane (bottom) switching. The LC molecules follow the reorientation of the azobenzene "command surface" to produce a change in intensity or phase of the incident light.

Computational modeling is a quick and cost effective alternative to trial and error synthesis. In the past, when scientists wanted to develop a new compound to serve their purposes, they would need to synthesize a large array of compounds. Not only can this work be resource intensive, but it also can be time-intensive as each synthesis and purification process can take weeks or even months. More recently, as computers have become more powerful, many researchers have been relying on computational chemical modeling to determine which proposed molecules would have favorable predicted results. Researchers then only have to synthesize the much smaller set of viable compounds rather than the large set containing every molecule. Computational modeling has already been used heavily by the pharmaceutical and optics industries to help synthesize new drugs and liquid crystals.

There are many different algorithms and methods available for chemical modeling, the fastest of which is semi-empirical. As the name suggests, this method relies on some previously obtained experimental data. Semi-empirical methods are very fast because they parameterize the calculation, but are not very accurate. Hartree-Fock is also a very common method. It is an *ab initio* method, meaning that it is not based on previous experimental data, but rather on simulations that are run from the beginning using physical principles. This method is extremely accurate, but also comes with a large computational cost.[3] Electron orbitals are expressed as one-electron functions, and the multi-electron calculation is based on the sum of the single-electron functions.[4] Density functional theory (DFT) and time-dependent density functional theory (TDDFT) try to provide a middle ground that is both fast and accurate. They use a 3-D electron density function rather than a many-electron wave function (Figure 3). TDDFT differs from DFT in that it accounts for how the system responds to an outside disturbance.

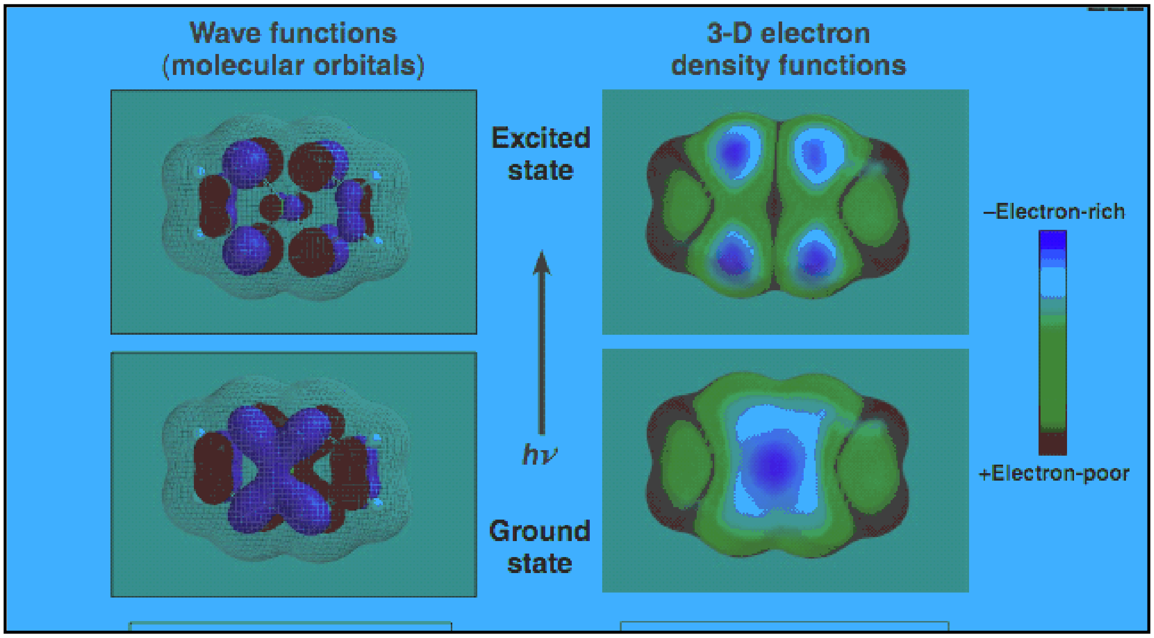

Fig. 3: A comparison of computed visualizations of wave functions vs electron density functions for the same molecule.

In this study, DFT and TDDFT were used to study the impact of molecular structure on optical switching properties in photoswitchable azobenzenes. Forty-two molecules were tested as possible components of photoalignment layers with low switching energies, enhanced bistability (the ability of a device or material to remain in one state indefinitely after the "writing" energy is removed), write/erase fatigue resistance, and high laser damage resistance.

2. Methodology

All calculations performed in this study were done using Schrödinger's Materials Science Suite software. The process is detailed in Fig. 4.

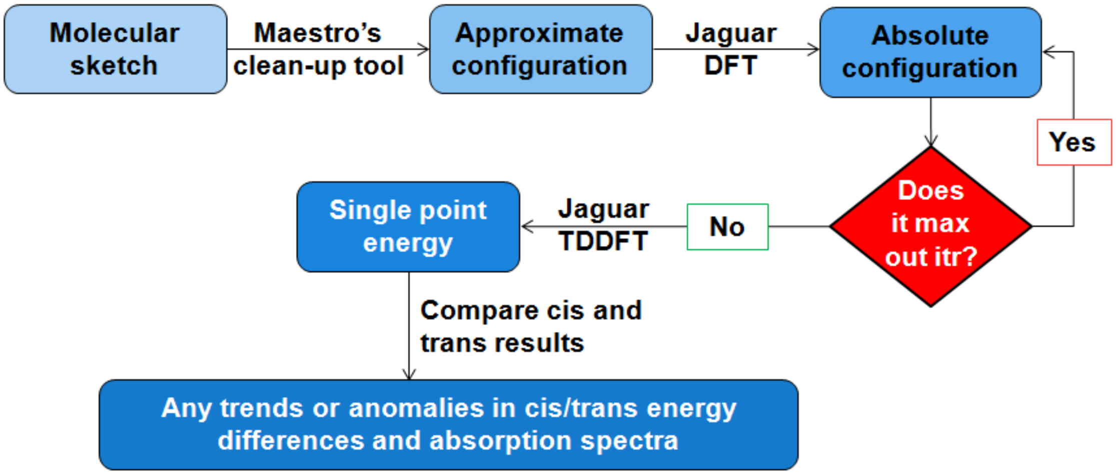

Fig. 4: Flowchart that portrays the methodology used in the computational analysis of candidate photoswitchable alignment layers employing azobenzenes.

Maestro is a visualization component of the Material Science Suite that allows the creation and visualization of molecules; it also includes a quick optimization routine that provides an approximate minimum-energy configuration of the molecular structure. Files generated by Maestro can be directly input into Jaguar computational engine for a more accurate geometry optimization using DFT. This optimization often had to be repeated as the molecules reach complexities at which they began to max out the iteration limits. Finally, the results of this optimization were input into TDDFT calculations that modeled the excited state absorption spectra.

One goal of the simulations was to find azobenzene structures that would impart high bistability to the photoswitchable alignment layer. In order for an azobenzene molecule to be bistable, there needs to be a significantly large difference between the activation energy required for it to undergo isomerization and the potential energies of the molecule in both its *cis* and *trans* states. However, if the energy barrier between the two states is too large, then optical switching will be difficult to achieve (Fig. 5).

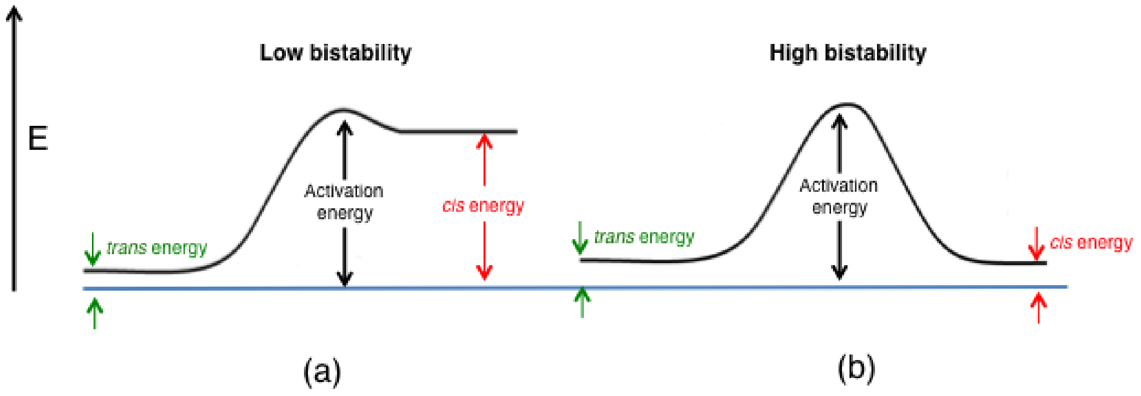

Fig. 5: Comparison of energy diagrams for photoswitchable azobenzene alignment layers. (a) a system with low bistability; the activation energy barrier required to switch from the *trans* state to the *cis* state is large, while the energy barrier for the reverse transition from *cis* to *trans* is relatively shallow, making conversion back to the *trans* isomer easy. (b) a system with high bistability; here, the energy barrier between both the *trans*-*cis* and *cis*-*trans* states is large, and once switched into the *cis* state the material will remain in that state indefinitely. The large activation energy barrier also means that a larger amount of optical energy will be needed to induce switching.

The initial model compound employed an alkyl spacer chain to tether a single azobenzene molecule with various kinds of terminal groups to a methacrylate *oligomer* (a "mini-polymer" with $\leq$ 10 to 15 repeat units); the example shown in Fig. 6 has an oligomeric backbone consisting of four repeat units of methacrylate groups. Computations were done using this short backbone rather than a fully polymerized chain to reduce the very large computational time and resources that would be required to compute energy levels for the complete polymer system.

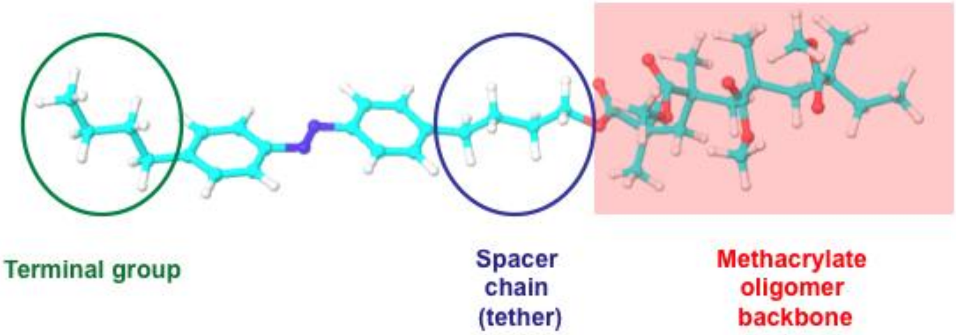

Fig. 6: An example of a single azobenzene repeat unit used in the simulations. This azobenzene contains a 4-carbon alkyl *terminal group* and is connected to the methacrylate oligomer on the right of the Figure by a 4-carbon spacer chain, or *tether*. A large number of these short backbones consisting of such "repeat units" would be linked together to form the polymer backbone by polymerization of the methacrylate groups at the ends of the oligomer chain.

3. Results and Discussion

Computational efforts focused on the effects of two different factors: (1) the length of the alkyl spacer chain (tether), and (2) the composition of the terminal group attached to the opposite end of the azobenzene structure (in Fig. 6, the 4-carbon chain on the left side of the molecule). Testing on the effects of spacer chain lengths was conducted with methoxy ($–OCH_3$) terminal groups to simplify the computations. Spacer chain lengths ranging from 1 to 12 were examined (Table 1). Figure 7 gives the difference between the *trans* and *cis* energies as a function of spacer length. At lengths of 4, 7, 10, and 12 there seem to be noticeable peaks in the difference in energies. In order to determine whether or not a pattern exists, however, additional alkyl spacer chain lengths need to be tested. One possible reason for the degradation of the pattern that seems to exist for spacer lengths 4, 7, and 10 is that the spacer chain eventually reached lengths (12 or higher) that are sufficiently long to began to fold itself into a convoluted shape, thus altering the energy values. Spacer chains of lengths 5, 6, 8, and 9 appear to be the best choices for azobenzenes designed to be bistable.

Spacer Length	*trans* Energy (hartrees)	*cis* Energy (hartrees)	Energy Difference (hartrees)	Energy Difference (kJ/mol)
1	-2149.203653	-2149.175137	0.028516	74.86874774
2	-2188.527937	-2188.50071	0.027227	71.48447871
3	-2227.843367	-2227.816239	0.027128	71.22455424
4	-2267.160542	-2267.12571	0.034832	91.45140347
5	-2306.474972	-2306.4509	0.024072	63.20102734
6	-2345.783562	-2345.762786	0.020776	54.54738053
7	-2385.110183	-2385.075182	0.035001	91.89511291
8	-2424.400884	-2424.375819	0.025065	65.80814849
9	-2463.734154	-2463.714671	0.019483	51.15260949
10	-2503.0624	-2503.031431	0.030969	81.30909836
11	-2542.366776	-2542.348358	0.018418	48.35645238
12	-2581.689842	-2581.6579	0.031942	83.86370951

Table 1: Calculated values of *trans*-*cis* isomerization energy for tethered azobenzenes with various spacer lengths. All materials had –OCH_3 as the terminal group.

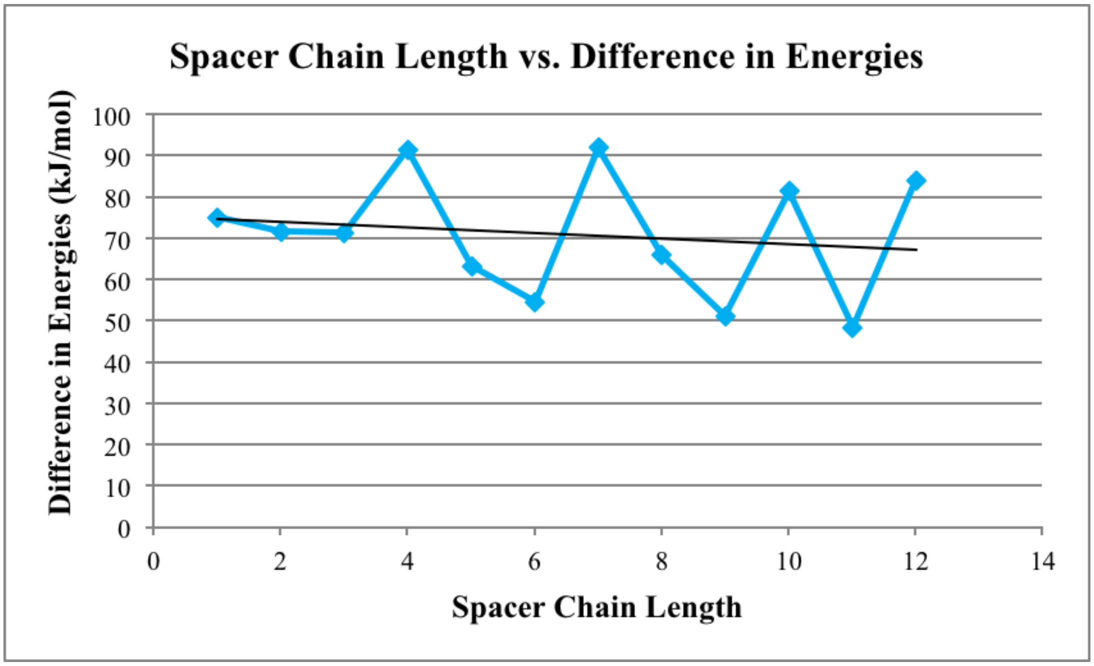

Fig. 7: Plot of the difference in energy between *trans* and *cis* states vs spacer chain length for the data shown in Table 1.

Alkyl chains ranging in length from 1 to 9 comprised a large portion of the terminal groups tested using the methods detailed earlier; the results are displayed below in Table 2 and Fig. 8.

Terminal group	*trans* Energy (hartrees)	*cis* Energy (hartrees)	Energy Difference (hartrees)	Energy Difference (kJ/mol)
Methyl	-2191.954981	-2191.920787	0.034194	89.7763347
Ethyl	-2231.27128	-2231.238445	0.032835	86.20828069
Propyl	-2270.588028	-2270.554955	0.033073	86.83314961
Butyl	-2309.903743	-2309.870307	0.033436	87.78620597
Pentyl	-2349.221007	-2349.187397	0.03361	88.24304291
Hexyl	-2388.537727	-2388.502606	0.035121	92.21017287
Heptyl	-2427.853855	-2427.817284	0.036571	96.01714735
Octyl	-2467.170722	-2467.133454	0.037268	97.8471206
Nonyl	-2506.486855	-2506.452856	0.033999	89.26436227

Table 2: Calculated values of *trans*-*cis* isomerization energy for tethered azobenzenes with various alkyl terminal group lengths.

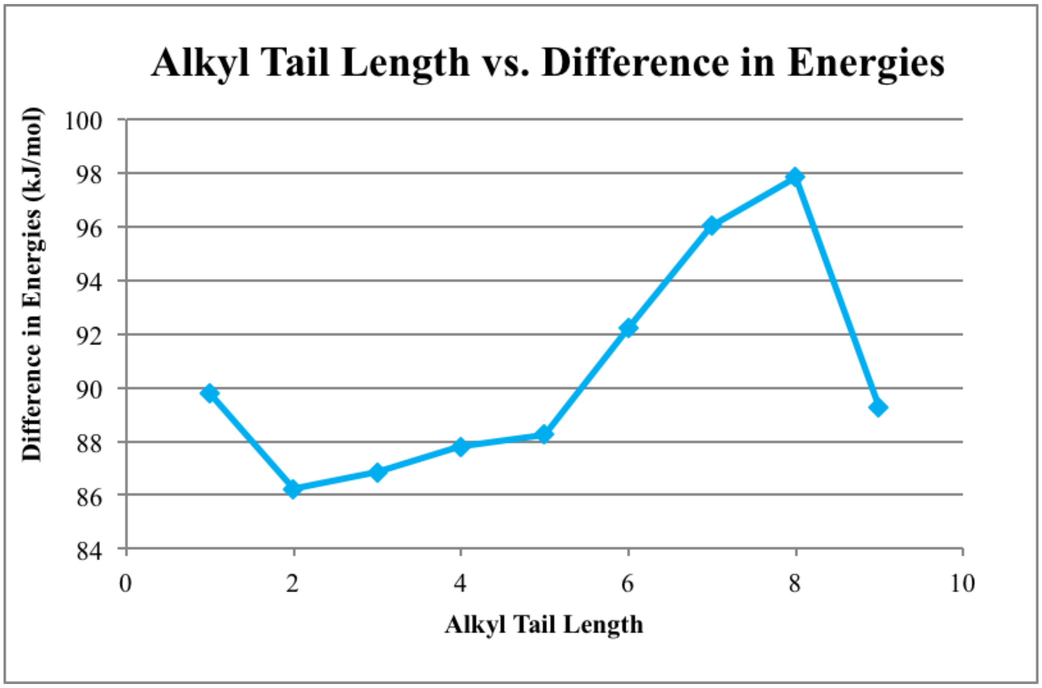

Fig. 8: Plot of the difference in energy between *trans* and *cis* states vs alkyl terminal group length for the data shown in Table 2.

These simulations clearly show that the energy difference increases steadily as the alkyl tail's length increases. The fact that the energy difference begins to decrease when the alkyl terminal group reaches a length of 9 can be attributed to folding of the carbon chain upon itself as was observed earlier for the alkyl tethering chains; the terminal groups contort themselves into a position that alters the chemical properties of the molecule significantly.

The remaining molecules that were tested contained a variety of other terminal groups, as well as some heteroaromatic rings. A complete listing of these terminal groups and the resulting *trans-cis* isomerization energies that result when they are attached to the azobenzene core can be seen in Tables 3 and 4. The energy differences between *trans* and *cis* isomers for the cyanate ester terminal group and the 2-methoxy-N-(2-methylphenyl) acetamide group were lower than that for an un-substituted azobenzene core by 16% and

72%, respectively. Additional work needs to be done, but this initial information points to terminal groups containing ester and acetamide functionalities as being potentially valuable for producing a bistable photoswitchable azobenzene. Chloromethyl acetamide, another terminal group in this class, was observed to increase the *trans-cis* isomerization energy difference by 43%.

Terminal group	***trans* Energy (hartrees)**	***cis* Energy (hartrees)**	**Energy Difference (hartrees)**	**Energy Difference (kJ/mol)**
None	-2152.634056	-2152.600728	0.033328	87.50265
Chloroalkane	-2612.228515	-2612.194726	0.033789	88.71301
Fluoroalkane	-2251.866129	-2251.832568	0.033561	88.11439
Trichloromethyl	-3570.708575	-3570.676345	0.03223	84.61985
Triflurormethyl	-2489.666375	-2489.636063	0.030312	79.58415
Cyanate ester	-2320.060921	-2320.033091	0.02783	73.06765
Isocyanate	-2320.116235	-2320.082803	0.033432	87.7757
Alcohol	-2227.855194	-2227.821613	0.033581	88.1669
2-methoxy-N-(2-methylphenyl) acetamide	-2706.243346	-2706.233957	0.009389	24.65082
Amine	-2207.994625	-2207.961011	0.033614	88.25354
Nitrile	-2244.875016	-2244.841972	0.033044	86.75701
Chloromethyl acetamide	-2820.248755	-2820.200977	0.047778	125.4411
NHOC2	-2360.652447	-2360.619731	0.032716	85.89585
CSSO2C	-3178.026333	-3177.994327	0.032006	84.03174

Table 3: Calculated values of *trans-cis* isomerization energy for tethered azobenzenes with a wide variety of terminal groups

Terminal group (rings)	***trans* Energy (hartrees)**	***cis* Energy (hartrees)**	**Energy Difference (hartrees)**	**Energy Difference (kJ/mol)**
6–membered	-2403.35558	-2403.321033	0.034547	90.70313608
5–membered	-2364.03914	-2364.005146	0.033994	89.25123477
Open 5–membered	-2365.23989	-2365.209427	0.030463	79.98059554

Table 4: Calculated values of *trans*-*cis* isomerization energy for tethered azobenzenes with heteroaliphatic rings as terminal groups.

The absorption spectra of the candidate molecules were calculated and analyzed; spectra for both the *cis* and *trans* isomers are shown in Figs. 9-18. The addition of terminal groups does not significantly alter the absorption spectra in most cases, which means that a narrow-band light source can be used to optically switch a wide variety of azobenzene photoalignment coatings. Only for the heteoraliphatic ring terminal groups was a bathochromic (red) shift in the absorption spectra observed.

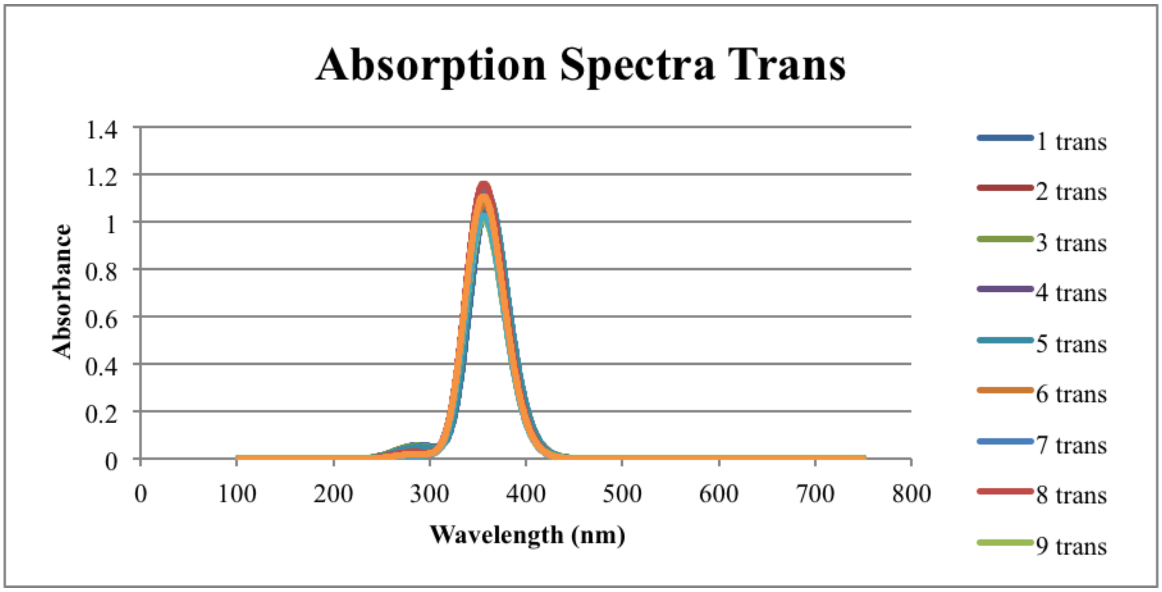

Fig. 9: Calculated absorption spectra for the *trans* isomer with spacer chain (tether) lengths ranging from 1-9.

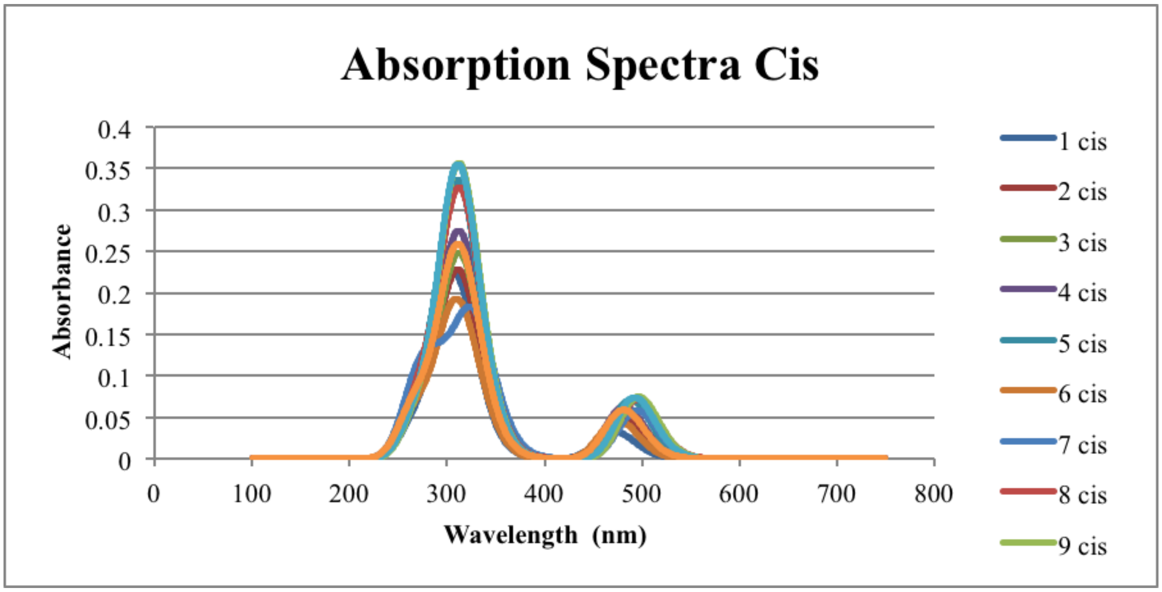

Fig. 10: Calculated absorption spectra for the *cis* isomer with spacer chain (tether) lengths ranging from 1-9.

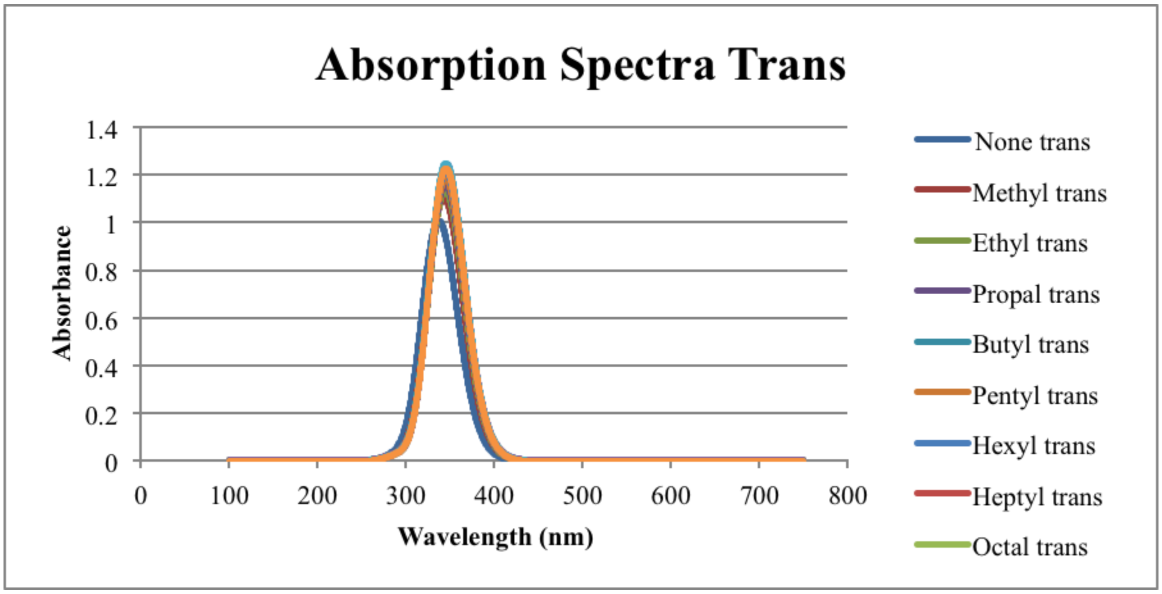

Fig. 11: Calculated absorption spectra for the *trans* isomer with alkyl terminal groups ranging from 1-8.

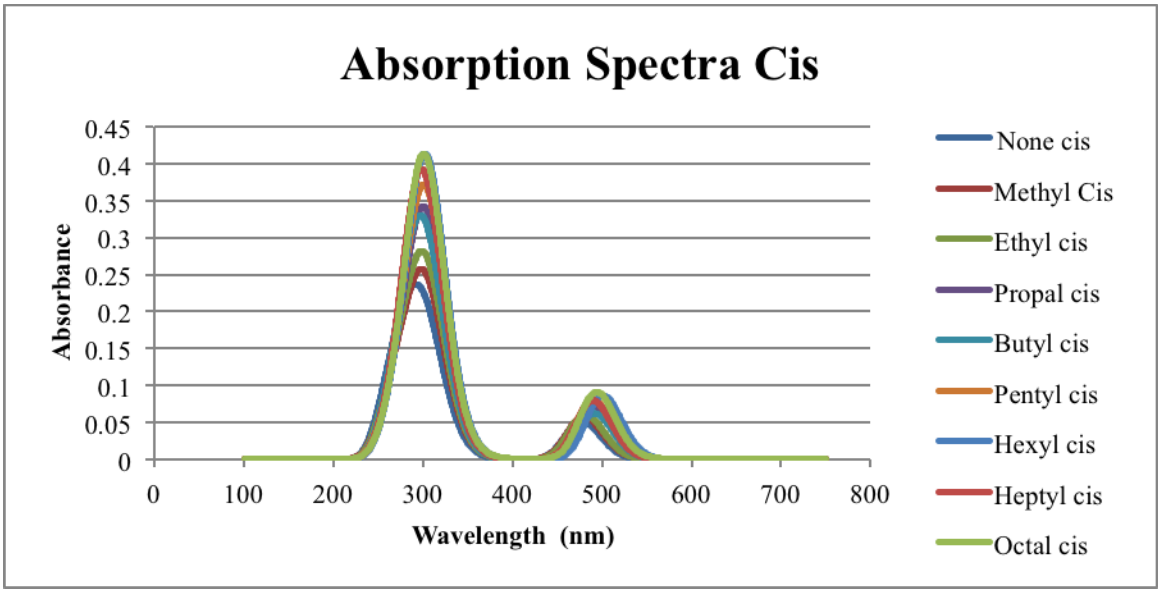

Fig. 12: Calculated absorption spectra for the *cis* isomer with alkyl terminal groups ranging from 1-8

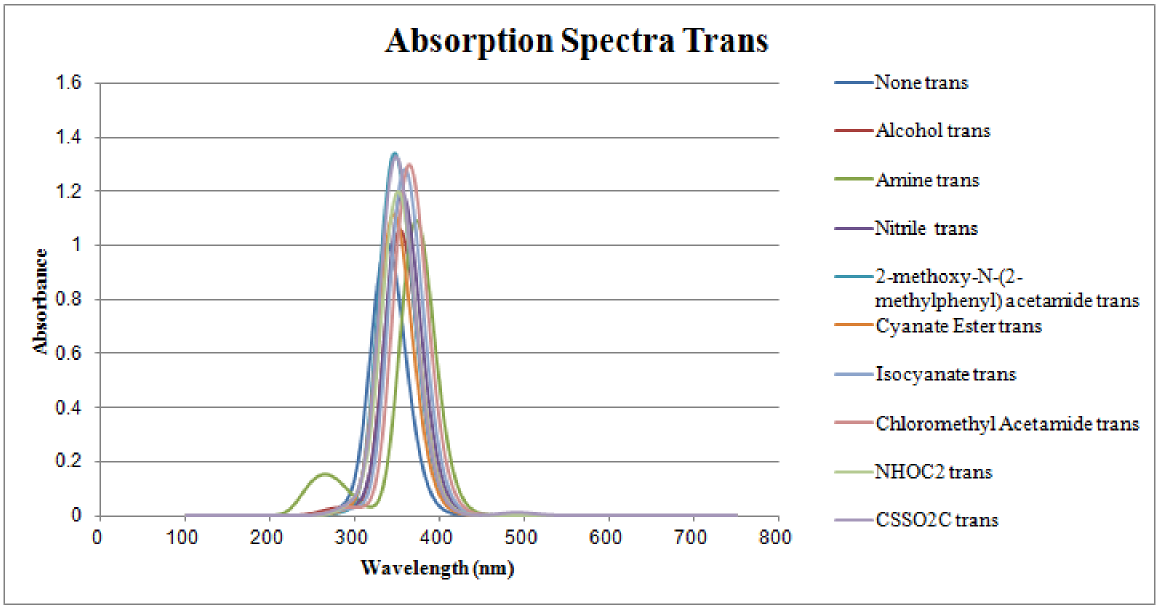

Fig. 13: Calculated absorption spectra for the *trans* isomer with various terminal groups

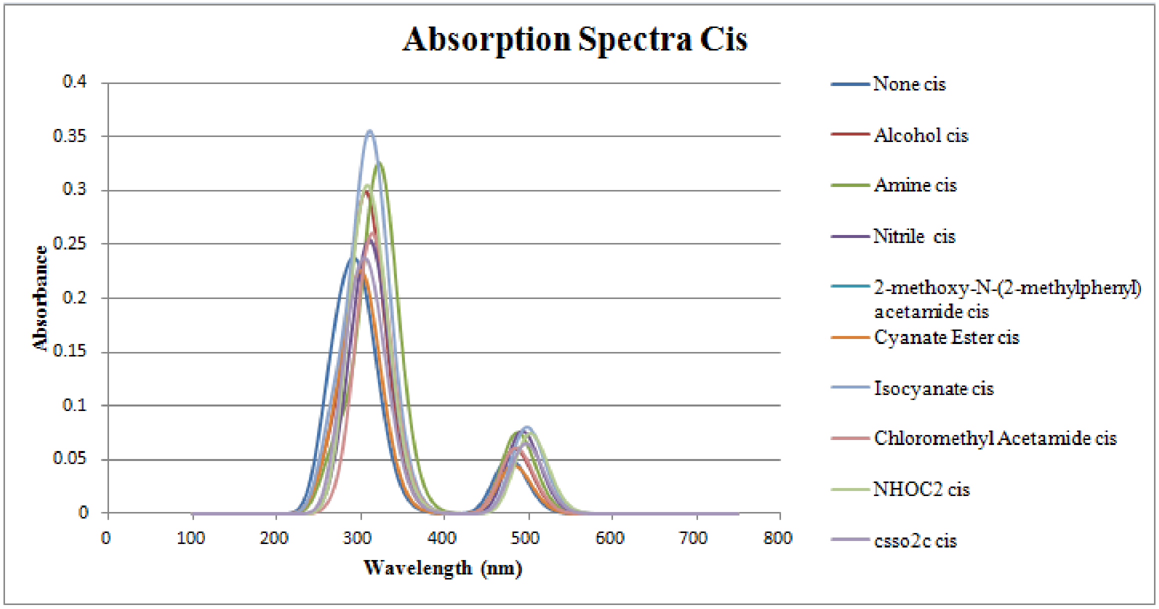

Fig. 14: Calculated absorption spectra for the *cis* isomer with various terminal groups.

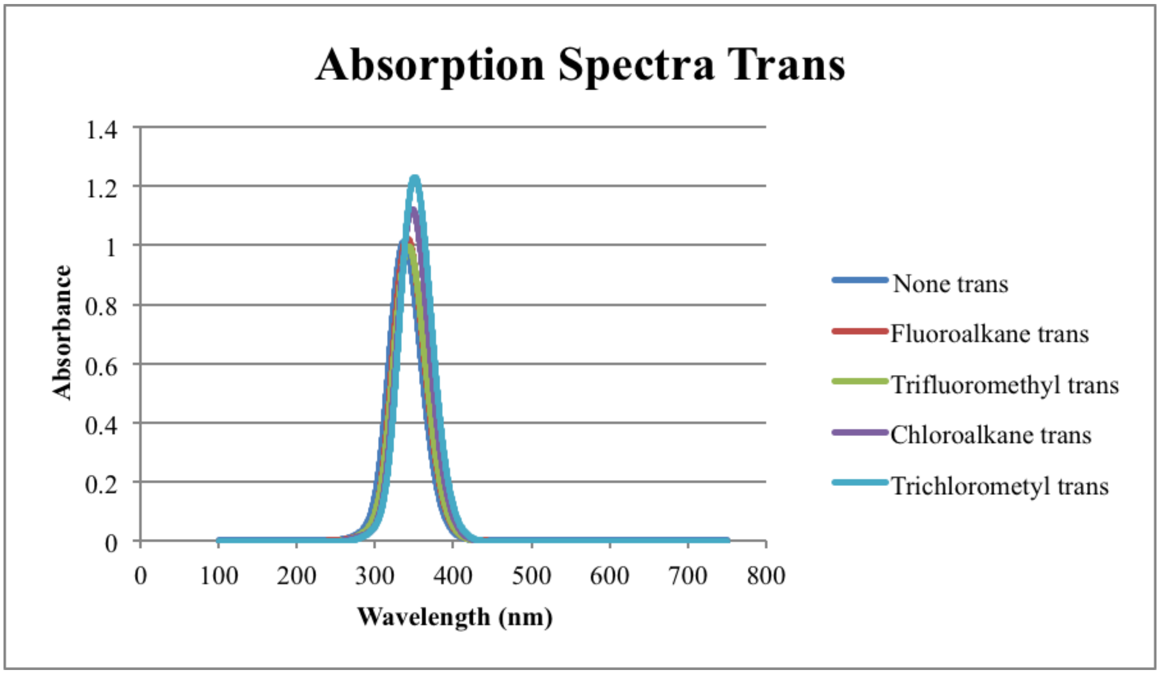

Fig. 15: Calculated absorption spectra for the *trans* isomer of azobenzenes with halogenated terminal groups

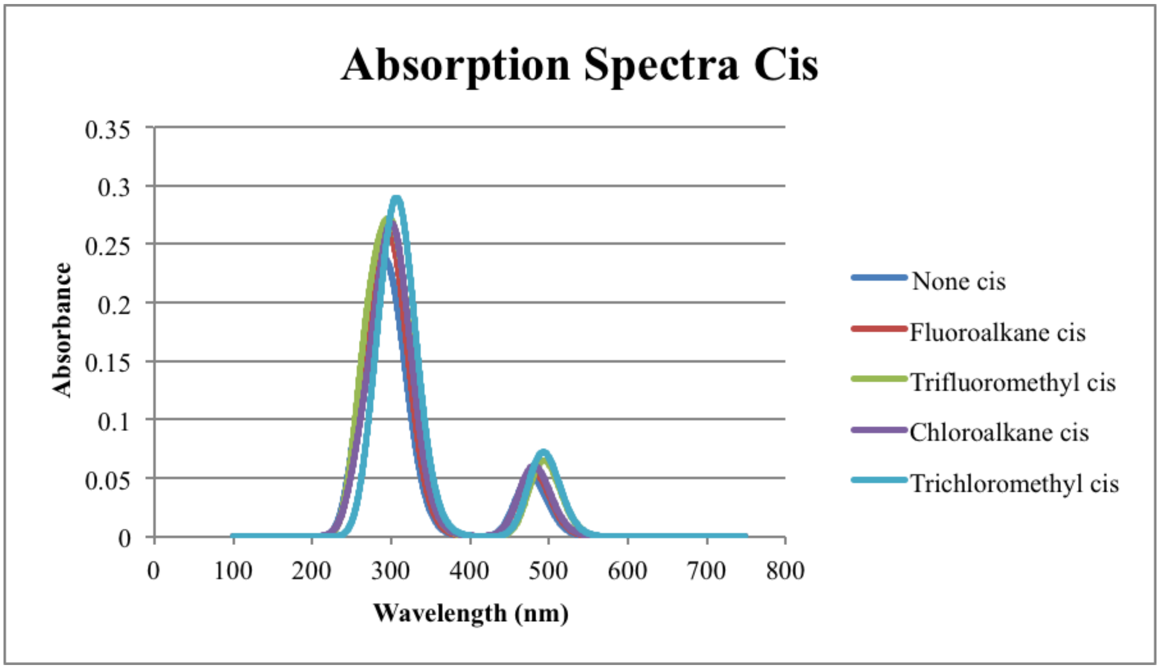

Fig. 16: Calculated absorption spectra for the *cis* isomer of azobenzenes with halogenated terminal groups.

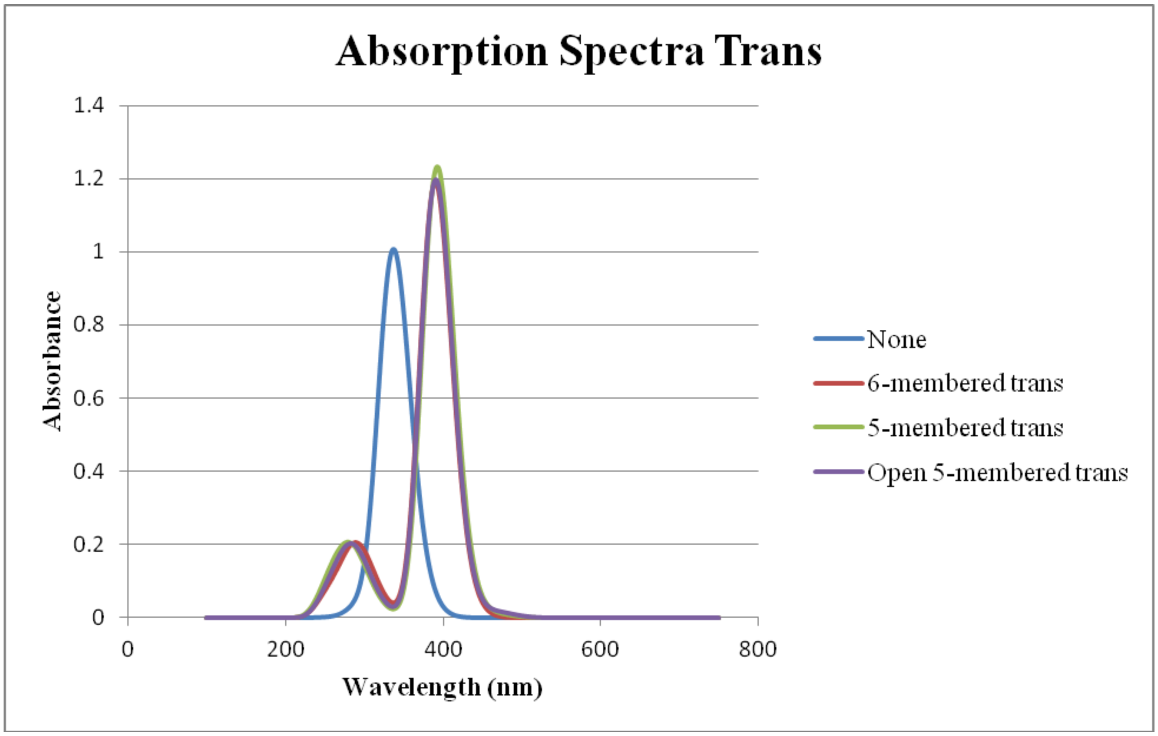

Fig. 17: Calculated absorption spectra for the *trans* isomer of various azobenzenes with terminal groups containing heteoaliphatic rings.

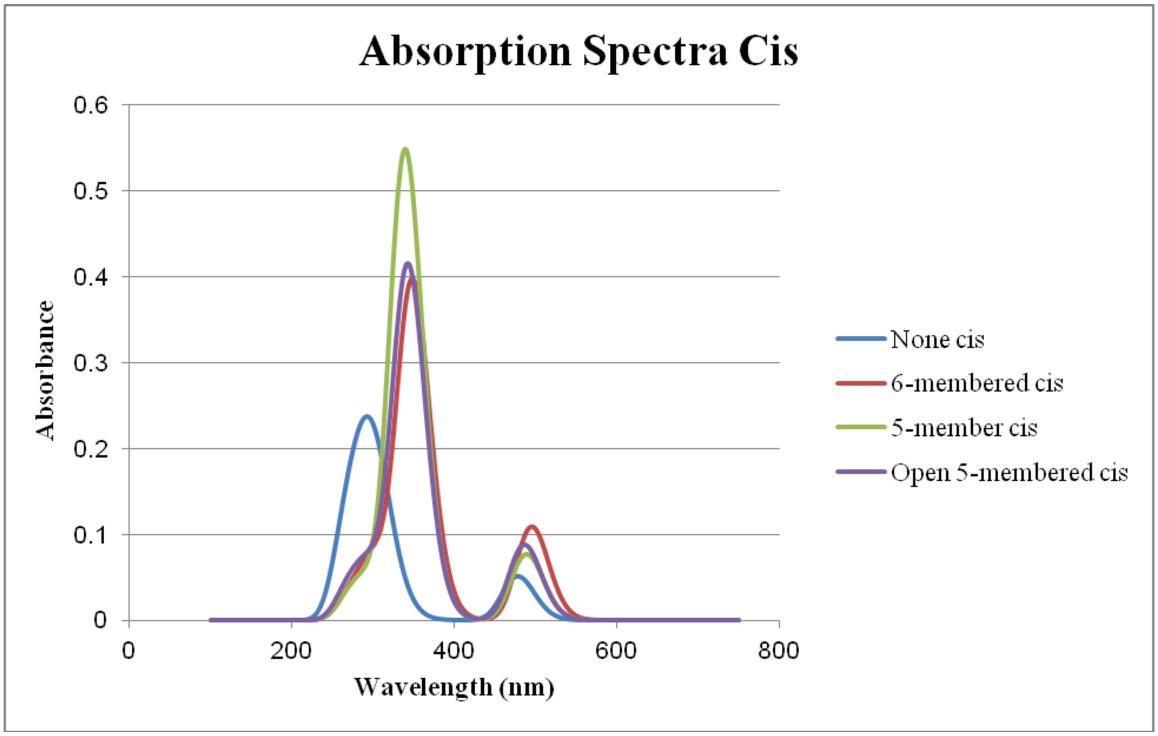

Fig. 18: Calculated absorption spectra for the *cis* isomer of various azobenzenes with terminal groups containing heteoaliphatic rings.

4. Conclusions

Using computational modeling, a azobenzene cores substituted with various terminal groups and tethered to a methacrylate oligomer by flexible alkyl chains were evaluated as potential candidates for photoswitchable alignment layers for an optically-switchable LC beam shaper. Both *trans-cis* isomerization energies and electronic absorption spectra for the various materials were calculated using Schrodinger's Materials Science Suite software using DFT and TDDFT computational methods. Alkyl spacer chains containing 5, 6, 8, and 9 carbons appear to be the optimal length for tethering the azobenzene to the methacrylate monomer to promote bistability; terminal groups containing ester and acetamide functionalities also appear to be valuable components in this regard. With the exception of heteroaromatic rings, most of the terminal groups evaluated did not significantly alter the calculated absorption spectra of the materials. Future investigations will center around the more computationally intensive task of conducting an in-depth study of the effect of the most favorable terminal groups and alkyl spacer chains determined in this preliminary study on the *trans-cis* isomerization energies in photoswitchable polymeric systems employing from 3 to 15 or more monomeric repeat units.

5. Acknowledgements

I thank Mr. Kenneth Marshall for his support and guidance in my research endeavor. I also thank Dr. R. Stephen Craxton for providing me with the opportunity to work at the University of Rochester's Laboratory for Laser Energetics. I also thank Emily Sekera in the Optical Materials group for working with me in running the simulations required for the completion of this project.

6. References

1. Marshall, K. L. et al., "Liquid crystal beam-shaping devices employing patterned photoalignment layers for high-peak-power laser applications," Proc. SPIE 8114, Paper 81140P, (2011).
2. Marshall, K. L. et al., "Liquid crystal near-IR laser beam shapers employing photoaddressable alignment layers for high-peak-power applications," Proc. SPIE 8828, Paper 88280N (2013).
3. Levine, Ira N. (1991*)*. Quantum Chemistry,: Prentice Hall, Englewood Cliffs, New Jersey , pp. 455–544.
4. Cramer, Christopher J. (2002). Essentials of Computational Chemistry. John Wiley & Sons Ltd ,Chichester, UK: pp. 153–189.